Acta Crystallographica Section D
Biological Crystallography
ISSN 0907-4449

Structure of BthA-I complexed with *p*-bromophenacyl bromide: possible correlations with lack of pharmacological activity

Angelo J. Magro,[a] Agnes A. S. Takeda,[a] Andreimar M. Soares[b] and Marcos R. M. Fontes[a]*

[a]Departamento de Física e Biofísica, Instituto de Biociências, UNESP, Distrito de Rubião Jr s/n, Caixa Postal 510, 18618-000 Botucatu-SP, Brazil, and [b]Departamento de Análises Clínicas, Toxicológicas e Bromatológicas, FCFRP, USP, Av. do Café s/n, 14040-903 Ribeirão Preto-SP, Brazil

Correspondence e-mail: fontes@ibb.unesp.br

Received 14 June 2005
Accepted 16 September 2005

PDB Reference: BthA-I–BPB complex, 1z76, r1z76sf.

The crystal structure of an acidic phospholipase A_2 isolated from *Bothrops jararacussu* venom (BthA-I) chemically modified with *p*-bromophenacyl bromide (BPB) has been determined at 1.85 Å resolution. The catalytic, platelet-aggregation inhibition, anticoagulant and hypotensive activities of BthA-I are abolished by ligand binding. Electron-density maps permitted unambiguous identification of inhibitor covalently bound to His48 in the substrate-binding cleft. The BthA-I–BPB complex contains three structural regions that are modified after inhibitor binding: the Ca^{2+}-binding loop, β-wing and C-terminal regions. Comparison of BthA-I–BPB with two other BPB-inhibited PLA_2 structures suggests that in the absence of Na^+ ions at the Ca^{2+}-binding loop, this loop and other regions of the PLA_2s undergo structural changes. The BthA-I–BPB structure reveals a novel oligomeric conformation. This conformation is more energetically and conformationally stable than the native structure and the abolition of pharmacological activities by the ligand may be related to the oligomeric structural changes. A residue of the 'pancreatic' loop (Lys69), which is usually attributed as providing the anticoagulant effect, is in the dimeric interface of BthA-I–BPB, leading to a new hypothesis regarding the abolition of this activity by BPB.

1. Introduction

Phospholipases A_2 (PLA_2s; EC 3.1.1.4) are small (~14 kDa), stable and ubiquitous enzymes. These molecules, which are present in biological fluids and cells, hydrolyze the *sn*-2 acyl groups of membrane phospholipids (*sn*-3 glycerophospholipids) to release fatty acids and lysophospholipids (van Deenen & de Haas, 1963). PLA_2s belong to a superfamily divided into 11 classes (Six & Dennis, 2000), five of which (I, II, III, V and X) are abundant in pancreatic secretions, inflammatory exudates and reptile and arthropod venoms (Rosenberg, 1990). In the genus *Bothrops*, PLA_2s from group IIB are the main components of the venoms produced by species classified into this animal group. In addition to their primary catalytic role, snake-venom PLA_2s show other important toxic/pharmacological effects including myonecrosis, neurotoxicity, cardiotoxicity and haemolytic, haemorrhagic, hypotensive, anticoagulant, platelet-aggregation inhibition and oedema-inducing activities (Gutiérrez & Lomonte, 1997; Ownby, 1998; Valentin & Lambeau, 2000). Some of these activities are correlated with the enzymatic activity, but others are completely independent (Kini & Evans, 1989; Soares & Giglio, 2003). It has been suggested that some specific sites in these molecules have biochemical properties that are responsible for the pharmacological and toxic actions, which

include anticoagulant and platelet-inhibition activities (Kini & Evans, 1989).

Several structural studies of PLA_2s complexed with inhibitors have recently been performed and have revealed correlations between their tertiary and quaternary structures and their biological effects (Watanabe *et al.*, 2005; Georgieva *et al.*, 2004; Chandra *et al.*, 2001). The crystal structure of bovine PLA_2 complexed with BPB (*p*-bromophenacyl bromide), a known inhibitor of the catalytic activity of PLA_2s, demonstrated that this enzyme was structurally modified by the ligand (Renetseder *et al.*, 1988). In contrast, Zhao *et al.* (1998) noted that the structure of an acidic PLA_2 from *Agkistrodon halys* Pallas (currently known as *Gloydius halys*) venom remained remarkably similar to the native structure after chemical modification by BPB.

Many non-catalytic (or with very low catalytic activity) homologous PLA_2s (Lys49-PLA_2s) have been purified from *Bothrops* snake venoms and have been structurally and functionally characterized (Watanabe *et al.*, 2005; Soares *et al.*, 2004; Magro *et al.*, 2003; Lee *et al.*, 2001; Arni *et al.*, 1999; da Silva-Giotto *et al.*, 1998; de Azevedo *et al.*, 1997). However, little is known about the bothropic catalytic PLA_2s (Asp49-PLA_2s) (Rigden *et al.*, 2003; Serrano *et al.*, 1999; Pereira *et al.*, 1998; Daniele *et al.*, 1995; Homsi-Brandeburgo *et al.*, 1988). BthA-I (an acidic PLA_2 isolated from *B. jararacussu* venom) is three to four times more active catalytically than BthTX-II (bothropstoxin-II from *B. jararacussu*) and other basic Asp49-PLA_2s from *Bothrops* venoms, but it is not myotoxic, cytotoxic or lethal (Andrião-Escarso *et al.*, 2002). Other activities demonstrated by this enzyme are time-independent oedema induction, hypotensive response in rats and platelet-aggregation inhibition (Andrião-Escarso *et al.*, 2002). These pharmacological effects as well as the catalytic and disintegrin activities were abolished by BPB, which covalently binds to residue His48 in the catalytic site (Andrião-Escarso *et al.*, 2002). Recently, we observed that BthA-I demonstrates anticoagulant activity, which is also abolished by BPB (data not shown). cDNA sequence cloning, functional expression, crystallization and X-ray diffraction data of BthA-I have also been described (Roberto, Kashima, Marcussi *et al.*, 2004; Roberto, Kashima, Soares *et al.*, 2004; Andrião-Escarso *et al.*, 2002). The crystal structure of native BthA-I has been recently described in two conformational states: monomeric (m-BthA-I) and dimeric (d-BthA-I) (Magro *et al.*, 2004).

In order to unambiguously define the structural basis of the BPB–Asp49-PLA_2 interaction, we present here the high-resolution structure of BthA-I chemically modified by BPB.

2. Material and methods

2.1. Isolation, cDNA cloning, sequencing and chemical modification

BthA-I was isolated from *B. jararacussu* snake venom by ion-exchange chromatography on CM-Sepharose followed by reverse-phase chromatography on an RP-HPLC C-18 column (Andrião-Escarso *et al.*, 2002). The amino-acid sequence of BthA-I was deduced from the cDNA sequence and deposited in GenBank (AY145836) (Roberto, Kashima, Marcussi *et al.*, 2004; Roberto, Kashima, Soares *et al.*, 2004). Modification of His48 with *p*-bromophenacyl bromide (BPB) was carried out as described previously (Andrião-Escarso *et al.*, 2002). *p*-Bromophenacyl bromide was purchased from Sigma Chemical Co.

Table 1
X-ray data-collection and refinement statistics.

Values in parentheses are for the highest resolution shell.

Unit-cell parameters (Å, °)	a = 41.0, b = 83.2, c = 45.6, β = 112.7
Space group	$P2_1$
Resolution (Å)	40.0–1.85 (1.95–1.85)
Unique reflections	22730 (3390)
Completeness (%)	94.4 (91.2)
R_{merge}† (%)	6.0 (37.1)
$I/\sigma(I)$	25.8 (3.5)
Redundancy	11.3 (5.6)
R_{cryst}‡ (%)	20.2 (28.9)
R_{free}§ (%)	25.1 (30.6)
No. of non-H atoms	
Protein	1900
Water	290
Mean B factor¶ (Å^2)	25.6
R.m.s. deviations from ideal values	
Bond lengths (Å)	0.034
Bond angles (°)	2.1
Ramachandran plot†† (%)	
Residues in most favoured region (%)	93.5
Residues in additional allowed region (%)	6.5
Residues in generously/disallowed regions (%)	0.0
Coordinate error¶ (Å)	
Luzzati plot [cross-validated Luzzati plot]	0.22 [0.28]
σ_A [cross-validated σ_A]	0.12 [0.15]

† $R_{merge} = \sum_{hkl}[\sum_i(|I_{hkl,i} - \langle I_{hkl}\rangle|)]/\sum_{hkl,i}\langle I_{hkl}\rangle$, where $I_{hkl,i}$ is the intensity of an individual measurement of the reflection with Miller indices h, k and l and $\langle I_{hkl}\rangle$ is the mean intensity of that reflection. Calculated for $I > -3\sigma(I)$. ‡ $R_{cryst} = \sum_{hkl}\big||F^{obs}_{hkl}| - |F^{calc}_{hkl}|\big|/|F^{obs}_{hkl}|$, where $|F^{obs}_{hkl}|$ and $|F^{calc}_{hkl}|$ are the observed and calculated structure-factor amplitudes. § R_{free} is equivalent to R_{cryst} but calculated with reflections (5%) omitted from the refinement process. ¶ Calculated with the program *CNS* (Brünger *et al.*, 1998). †† Calculated with the program *PROCHECK* (Laskowski *et al.*, 1993).

2.2. Crystallization and X-ray data collection

Lyophilized samples of BthA-I–BPB were dissolved in ultrapure water at a concentration of 10 mg ml^{-1}. A sparse-matrix method (Jancarik & Kim, 1991) was utilized to perform initial screening of the crystallization conditions because crystallization experiments using the original conditions for native BthA-I were unsuccessful. Crystals of BthA-I–BPB were obtained by the conventional hanging-drop vapour-diffusion method (MacPherson, 1982) in which the protein solution was equilibrated against a reservoir solution containing 0.2 *M* magnesium chloride, 32%(*w*/*v*) polyethylene glycol 4000 and 0.1 *M* Tris–HCl pH 8.5 as described previously (Takeda *et al.*, 2004). The best crystals measured approximately 0.4 × 0.3 × 0.2 mm after 10–14 d at 291 K. After mounting the crystal in a nylon loop and flash-freezing it in a nitrogen stream at 100 K with no cryoprotectant, X-ray diffraction data were collected at a wavelength of 1.38 Å using a synchrotron-radiation source (LNLS, Campinas, Brazil) and a MAR CCD imaging-plate detector (MAR Research). Data

were processed to 1.85 Å resolution using *DENZO* and *SCALEPACK* (Otwinowski & Minor, 1997). The data set was 94.4% complete at the highest resolution with R_{merge} = 6.0%. The space group was $P2_1$. Data-processing statistics are presented in Table 1.

2.3. Structure determination and refinement

The BthA-I–BPB crystal structure was solved by molecular replacement using *AMoRe* (Navaza, 1994) with the coordinates of native monomeric BthA-I (PDB code 1umv) as the search model (Magro *et al.*, 2004). After a cycle of simulated-annealing refinement using *CNS* (Brünger *et al.*, 1998), the electron-density maps were inspected using *O* (Jones *et al.*, 1990) and the chemically modified residue His48/BPB of the acidic PLA_2 from *A. halys* Pallas venom (PDB code 1bk9) (Zhao *et al.*, 1998) was inserted in the structure to substitute the original His48 from native BthA-I. Electron-density maps calculated with $3|F_{obs}| - 2|F_{calc}|$ coefficients and simulated-annealing omit maps calculated with analogous coefficients were generally used. The model was improved, as judged by analysis of the free *R* factor (Brünger *et al.*, 1998), through rounds of crystallographic refinement (positional and restrained isotropic individual *B*-factor refinement, with an overall anisotropic temperature factor and bulk-solvent correction) and manual rebuilding. Three mutations were made because of the lack of electron density in some regions of the protein (Glu16→Gly in monomer *A*; Glu16→Gly, Lys78→Gly and Lys123→Gly in monomer *B*). The dictionaries of residue His48/BPB used by *CNS* (Brünger *et al.*, 1998) and *O* (Jones *et al.*, 1990) were generated using the programs *XPLO2D* and *MOLEMAN*2 (Kleywegt & Jones, 1997). Solvent molecules were added and refined using *CNS* (Brünger *et al.*, 1998).

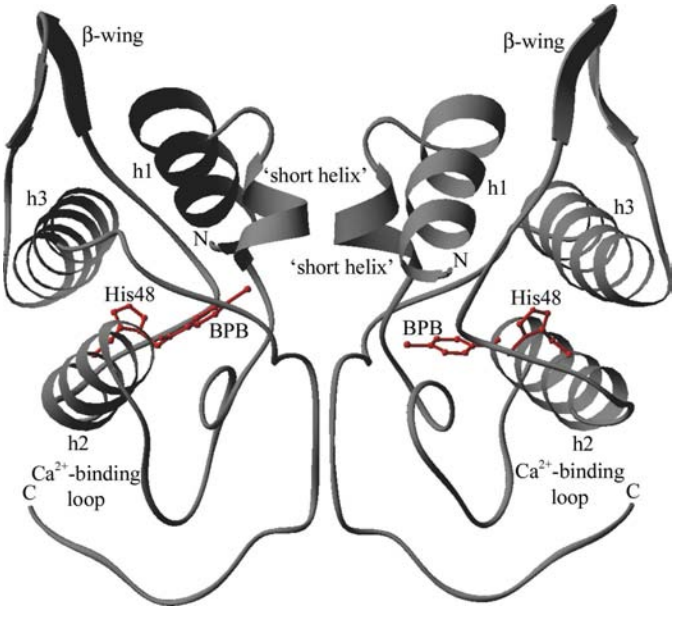

Figure 1
The structure of BthA-I complexed with BPB is shown as a ribbon diagram (Carson, 1997).

The refinement converged to *R* and R_{free} factors of 20.2 and 25.1%, respectively (see Table 1 for definition of *R* factors), and the final model comprises 1900 non-H protein atoms and 290 water molecules (Table 1). *O* (Jones *et al.*, 1990) was used for molecular superposition of the PLA_2 structures using only the C^{α} coordinates. The stereochemistry of the final structure was evaluated using *PROCHECK* (Laskowski *et al.*, 1993).

3. Results

3.1. Overall structure of the BthA-I–BPB complex

The crystals of the BthA-I–BPB complex diffract to 1.85 Å and are monoclinic, belonging to space group $P2_1$ with unit-cell parameters a = 41.0, b = 45.6, c = 83.2 Å, β = 112.7°. The refinement converged to a crystallographic residual of 20.2% (R_{free} = 25.1%) for all data between 27.15 and 1.85 Å (Table 1). The structure shows excellent overall stereochemistry, with no residues found in the disallowed or generously allowed regions of the Ramachandran plot. The overall *PROCHECK* *G* factor is −0.1 (Laskowski *et al.*, 1993).

BthA-I–BPB is a dimeric structure with seven disulfide bridges in each monomer and like other class II PLA_2s has the following structural features: (i) an N-terminal α-helix, (ii) a 'short' helix, (iii) a Ca^{2+}-binding loop, (iv) two antiparallel α-helices (2 and 3), (v) two short strands of antiparallel β-sheet (β-wing) and (vi) a C-terminal loop (Fig. 1). The catalytic network for class II PLA_2s, formed by His48, Tyr52, Tyr73 and Asp99, is fully conserved.

The monomers of BthA-I–BPB are related by an approximate twofold axis parallel to the 'short' helix (Fig. 1). Hydrophobic contacts and three intermolecular hydrogen bonds contribute to the stabilization of the dimer. The contacts involve residues of both N-termini (Leu2, Trp3 and Lys7), both C-termini (Trp118, Phe119), the 'short' helices (Leu20, Gln21) and the 'pancreatic' loops located between α-helix 2 and the β-wing (Lys69) (Fig. 2). Furthermore, the Br atom of the BPB group from monomer *A* interacts with the Phe119 (C-terminal region) of monomer *B*.

A BPB molecule is covalently bound to the $N^{\delta1}$ atom of His48 of both monomers as illustrated in Fig. 3. The catalytic water hydrogen bonded to His48 $N^{\delta1}$ present in the native BthA-I structure is not present in the current structure and in both monomers the His48 imidazole ring is in the same position (Fig. 4) as observed in the native structure. The conformations of all residues involved in the catalytic network (Scott *et al.*, 1990) are structurally conserved in the native and inhibited structures, with the exception of Gly30 in monomer *A* (Fig. 4*a*).

The phenacyl group of BPB molecule extends along the hydrophobic substrate-binding channel of the protein, making several hydrophobic interactions (Fig. 5). The inhibitors in both monomers interact with Cys45 and Gly30. Additionally, the BPB molecules make other specific contacts: in monomer *A* with Phe119 (from monomer *B*) and two water molecules and in monomer *B* with Phe5 and Tyr22.

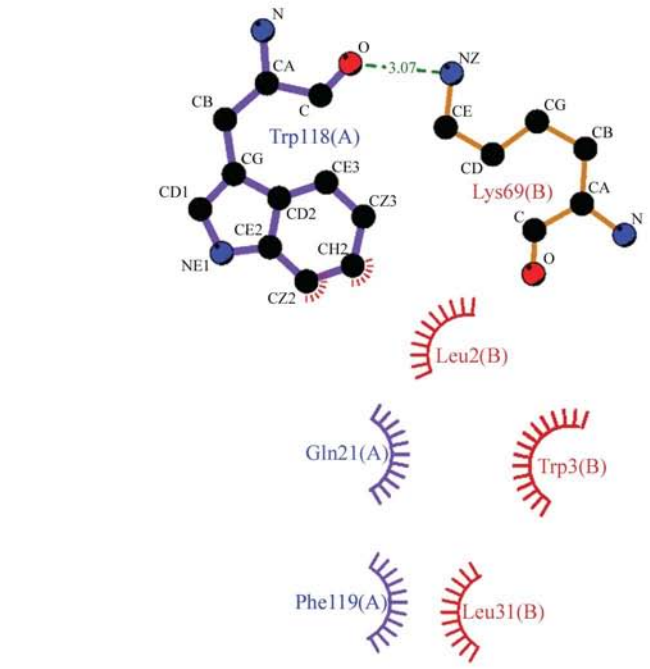

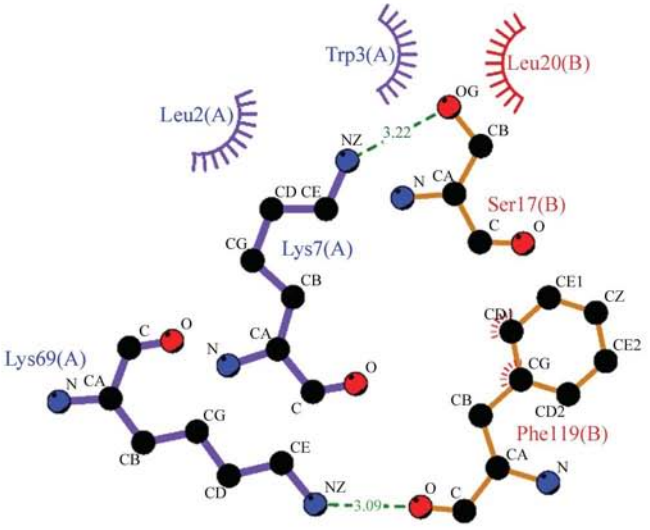

Figure 2
Schematic diagram of the dimer–interface interactions. Polar contacts are shown with dashed lines and hydrophobic contacts are indicated by arcs with radiating spokes. Monomer *A* residues are shown with purple bonds and are labelled in blue and monomer *B* residues are shown with gold bonds and are labelled in red. C, N and O atoms are shown in black, blue and red, respectively. This figure was prepared using the program *DIMPLOT* (Wallace *et al.*, 1995).

3.2. Comparison of native BthA-I and BthA-I–BPB complex

Table 2 catalogues the r.m.s. deviations after superposition of five BthA-I monomers (m-BthA-I and both monomers of d-BthA-I and BthA-I–BPB). This comparison shows the effect of the BPB molecule on the tertiary structure of BthA-I. The m-BthA-I and d-BthA-I monomers are more similar, with an r.m.s. deviation of about 0.5 Å between C^{α} atoms. In contrast, comparison of structures with and without BPB gives r.m.s. deviations of approximately 1.2 Å.

Fig. 6 shows the superposition of the three main helices (h1, h2 and h3) of m-BthA-I and monomer *A* of BthA-I–BPB and d-BthA-I. This comparison indicates that there are two main regions with significant structural differences: the Ca^{2+}-binding loop and the β-wing. Additionally, there are also structural changes in the C-terminal region.

Superposition of the BthA-I–BPB monomers resulted in an r.m.s. deviation between C^{α} atoms of 0.72 Å, while the same superposition between native d-BthA-I monomers resulted in a value of 0.54 Å. These results are similar to those obtained for other dimeric PLA_2s (Magro *et al.*, 2003).

In order to understand the quaternary structure changes between BPB-inhibited and native d-BthA-I, monomer *A* from both structures were superposed (C^{α} atoms of α-helices h1, h2 and h3 were used in the superposition) to determine the relative disposition of monomers *B* (Fig. 7). In the BPB-inhibited structure a completely new dimer interface is observed.

4. Discussion

4.1. Structural comparison of native and inhibited BthA-I

Comparison of the monomers of BPB-inhibited and native d-BthA-I and m-BthA-I results in the observation of three

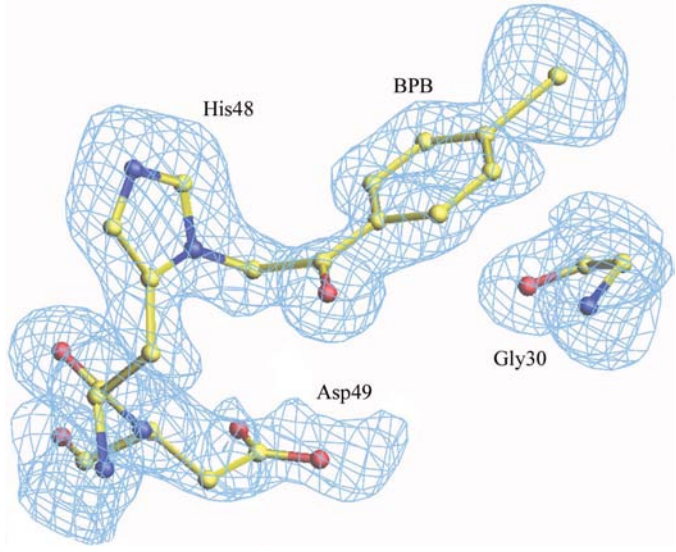

Figure 3
$3|F_{obs}| - 2|F_{calc}|$ electron-density omit map in the catalytic site region of monomer *A* of the BthA-I–BPB complex showing the His48 residue covalently bound with BPB contoured at 1.5 standard deviations. This figure was generated using *O* (Jones *et al.*, 1990).

Table 2
Superposition between BthA-I monomers (r.m.s. deviation of C^{α} atoms in Å).

	BthA-I–BPB		d-BthA-I		
	Monomer *A*	Monomer *B*	Monomer *A*	Monomer *B*	m-BthA-I
BthA-I–BPB (monomer *A*)	—	0.72	1.23	1.21	1.26
BthA-I–BPB (monomer *B*)	0.72	—	1.21	1.23	1.17
d-BthA-I (monomer *A*)	1.23	1.21	—	0.54	0.49
d-BthA-I (monomer *B*)	1.21	1.23	0.54	—	0.49
m-BthA-I	1.26	1.17	0.49	0.49	—

main regions with significant structural differences: the Ca^{2+}-binding loop (residues 27–37), the β-wing (residues 75–84) and the C-terminal region (residues 119–133) (Fig. 6). It has been shown these regions are the most variable between the class I and II PLA_2s (Magro *et al.*, 2004).

The presence of the inhibitor in the active site displaces the Ca^{2+}-binding loop, which interacts with the C-terminal region, which is also displaced. Residues Gly30, Leu31 and Leu32 are displaced by the BPB group, yielding a different conformation of the Ca^{2+}-binding loop. Comparison of monomer *B* of BthA-I–BPB with the m-BthA-I and d-BthA-I monomers indicates significant structural modification of the Gly32 main chain and Leu31 main and side chains, while the same comparison for monomer *A* shows that not only the Gly32 and Leu31 but also the Gly30 main-chain atoms were displaced. Additionally, Leu23 from the 'short' helix is also displaced by the BPB group. Despite the disulfide bridge between Cys133 and Cys50 which gives reasonable stability to the C-terminal region, residues 123–130 are shifted up to 2.6 Å compared with the native BthA-I structure.

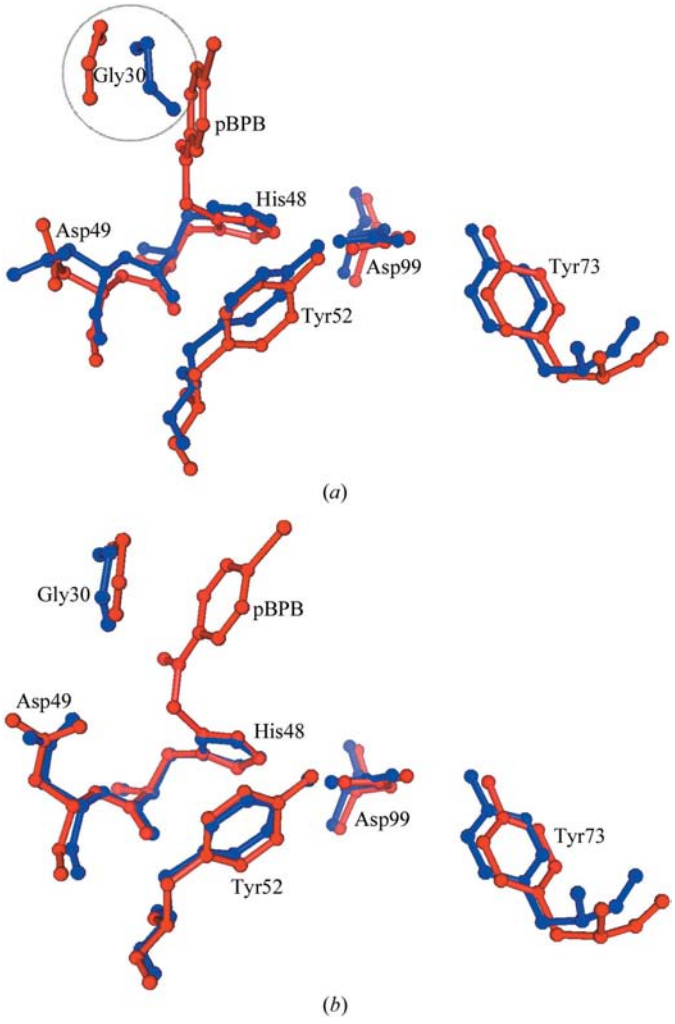

Figure 4
Superposition of residues involved in the catalytic network (Scott *et al.*, 1990). (*a*) Residues Gly30, His48, Asp49, Tyr52, Tyr73 and Asp99 of monomer *A* of native d-BthA-I (blue) and of the complex BthA-I–BPB (red) were superimposed. The C^{α} atoms of α-helices h1, h2 and h3 were used in the superposition. (*b*) Superposition of the catalytic residues of monomer *B* of native d-BthA-I (blue) and of the complex BthA-I–BPB (red) superimposed as in (*a*). This figure was drawn using *PyMol* (DeLano, 2002).

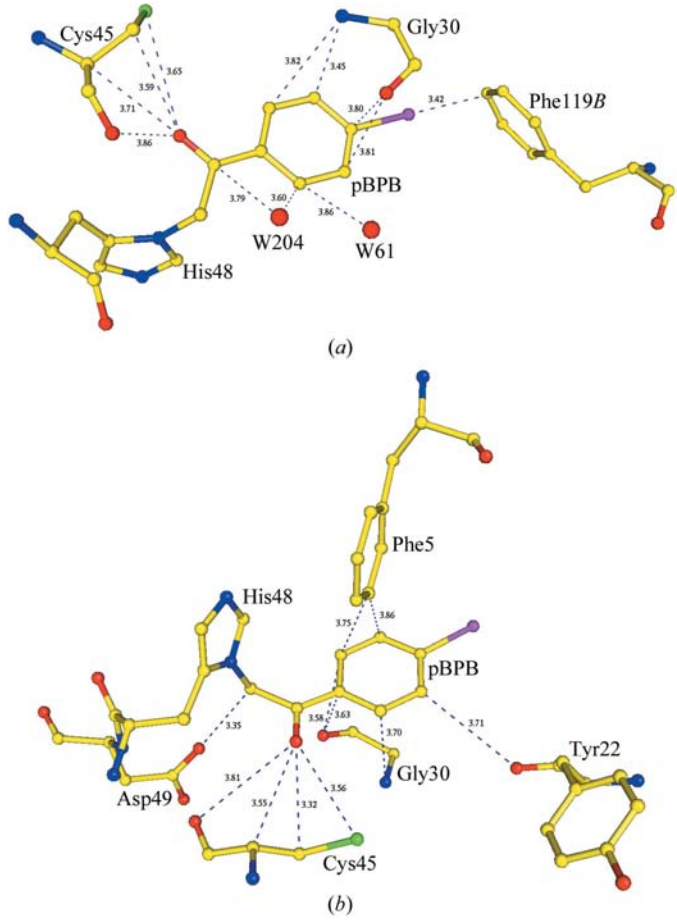

Figure 5
BPB-group interaction with the residues of the BthA-I–BPB complex structure. (*a*) Monomer *A* interactions. Residues Gly30, His48, Cys45 and Phe119 (from monomer *B*) and two water molecules (W61 and W204) are labelled (red, oxygen; yellow, carbon; blue, nitrogen; green, sulfur; pink, bromide). (*b*) Monomer *B* interactions. Residues Phe5, Tyr22, Gly30, His48, Asp49 and Cys45 are labelled (colored as in *a*). This figure was drawn using *RIBBONS* (Carson, 1997).

The BthA-I–BPB structure reveals a novel oligomeric conformation compared with d-BthA-I and with all class IIA PLA_2 structures available in the PDB. The dimer of d-BthA-I (Fig. 7) is stabilized by only a few hydrophobic contacts (six interactions), a salt bridge between Lys93 N^{ε} and Glu108 $O^{\delta 2}$ and an additional interaction of Lys93 with Thr104. In contrast, the dimer of BthA-I–BPB is stabilized by a larger number of hydrophobic contacts (12 interactions) and three intermolecular hydrogen bonds. In addition, the BPB group of monomer *A* interacts with the C-terminus of monomer *B* (Phe119) (Fig. 5*a*). The dimeric interface of BthA-I–BPB includes different regions of the protein: the C-terminal, N-terminal, 'short' helix and 'pancreatic' loop; in BthA-I the dimer contacts only involve the β-wing and α-helix h3. Furthermore, BthA-I–BPB is a more compact structure compared with BthA-I, as observed by calculating the buried surface between the monomers in the dimer: 1706 Å^2 for BthA-I–BPB and 1044 Å^2 for d-BthA-I. If all of the reasons above (number of interactions, parts of protein involved in the contacts and buried surface) are taken into account, we can hypothesize that the oligomeric structure of BthA-I–BPB is more stable than that of the native protein.

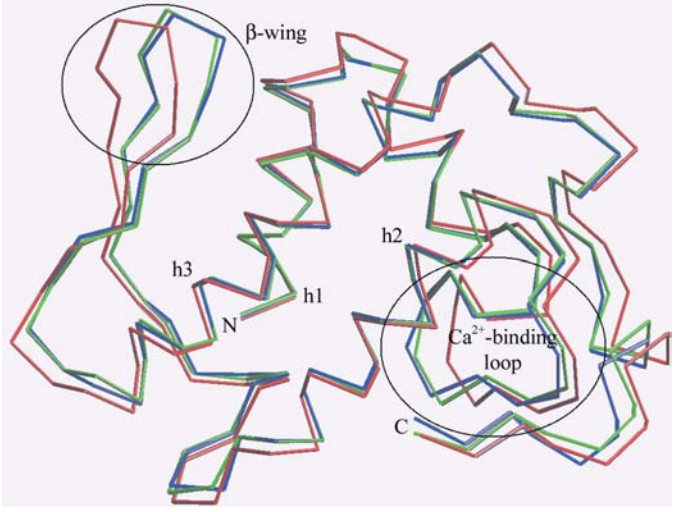

Figure 6
Superposition between BthA-I–BPB monomer *A* (red), m-BthA-I (green) and d-BthA-I monomer *A* (blue). The C^{α} atoms of α-helices h1, h2 and h3 were used in the superposition. This figure was generated using *O* (Jones *et al.*, 1990).

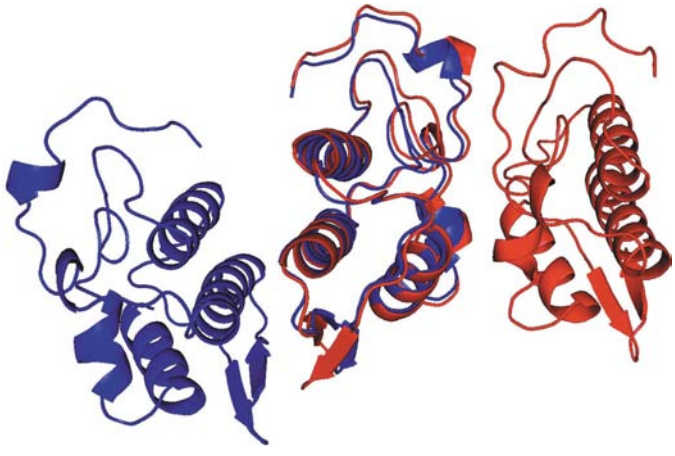

Figure 7
Superposition of monomer *A* from BthA-I–BPB (red) and d-BthA-I (blue) with the relative disposition of monomer *B*. The C^{α} atoms of α-helices h1, h2 and h3 were used in the superposition. This figure was drawn using *PyMol* (DeLano, 2002).

The alternative oligomeric conformation of BthA-I–BPB may be related to the structural changes which accompany BPB binding, mainly in the C-terminal region, leading to a more energetically stable structure. Additionally, the change in the physicochemical parameters used in the crystallization experiments (for example, pH 8.5 for BthA-I–BPB and pH 3.5 for d-BthA-I) may have affected the fragile stabilization of d-BthA-I described by Magro *et al.* (2004). In contrast, the conformational change of the β-wing region is probably a consequence of higher mobility of this region. The β-wing's average *B* factor is 32.9 Å^2, while for the entire structure this value is 24.5 Å^2. The β-wing is a region known to be highly flexible in class II PLA_2 enzymes (Magro *et al.*, 2003; da Silva-Giotto *et al.*, 1998). BPB binding probably does not directly affect the β-wing conformation because it is shielded by two α-helices (h2 and h3) which have relatively low mobility (the average *B* factors for the h2 and h3 helices are 19.6 and 21.3 Å^2, respectively).

In the Asp49-PLA_2 piratoxin III structure (Rigden *et al.*, 2003), the Ca^{2+}-binding loop exhibits significant structural distortion when compared with other PLA_2s owing to an extreme diversion taken by the main chain of residues 30–31 which is associated with a change in the backbone dihedral angles of Cys29. The authors suggest this distortion may be a consequence of an alternative conformation of the enzyme (T-state). Following the reasoning of these authors, the BthA-I and BthA-I–BPB structures would represent R-state and T-state conformations, respectively.

4.2. Structural comparison between the inhibited PLA_2s

The crystal structure of bovine pancreatic PLA_2 complexed with BPB (Renetseder *et al.*, 1988) revealed both a Ca^{2+}-binding loop and a 'pancreatic' loop (residues 59–72) with structural differences compared with the native protein. In contrast, the crystal structure of acidic PLA_2 from *A. halys* Pallas venom complexed with BPB (Zhao *et al.*, 1998) showed remarkable similarity to the native structure (the r.m.s. deviation of C^{α} atoms is 0.243 Å). The crystal structures of PLA_2s complexed with BPB represent apparently paradoxical results: one induces structural changes in parts of structure and the other does not (Renetseder *et al.*, 1988; Zhao *et al.*, 1998). These results might initially be attributed to structural differences in the native proteins, which belong to different species and classes of PLA_2s; however, closer study suggests these differences may be attributed mainly to the presence of Na^+ ion at the Ca^{2+}-binding loop.

Comparison of the BPB-inhibited and native BthA-I leads to the observation of three main regions with significant structural differences: the Ca^{2+}-binding loop, the C-terminus

and the β-wing. In addition, analysis of the two inhibited PLA_2 structures (BthA-I–BPB and bovine pancreatic PLA_2) shows that BPB binding causes changes in the conformational structure of the Ca^{2+}-binding loop while for BPB-inhibited *A. halys* Pallas PLA_2, whose Ca^{2+}-binding loop binds an Na^+ ion (Zhao *et al.*, 1998), it did not cause significant changes. It has been suggested that divalent cations such as Ca^{2+} protect bovine PLA_2 against inactivation by BPB and that Ca^{2+} does not bind to the inactivated PLA_2 (Volwerk *et al.*, 1974). Similarly, acidic PLA_2 from *A. halys* Pallas in the presence of Ca^{2+} prevents BPB modification (Zhang *et al.*, 1994). This is probably a consequence of the absence of a water molecule that coordinates the Ca^{2+} ion which was displaced by the BPB group (Renetseder *et al.*, 1988; Zhao *et al.*, 1998). However, the incomplete Ca^{2+} coordination by the ligands creates a distorted geometry of the Ca^{2+}-binding loop. This new arrangement still may accommodate an Na^+ ion in the loop and keeps it in a similar conformation to that observed by Zhao *et al.* (1998). These authors also observed that the presence of an Na^+ ion may be related to the minor conformational changes in structure. Consequently, we suggest that PLA_2s undergo structural changes when chemically modified with BPB, particularly at the Ca^{2+}-binding loop, leading to loss of catalytic activity.

4.3. Inhibition of pharmacological activity by BPB

Phospholipases A_2 from snake venoms are intriguing proteins with a wide range of pharmacological effects in addition to their catalytic role. Kini & Evans (1989) proposed a model in which there are specific pharmacological sites in different parts of the protein. However, in terms of structural information, little is known about the precise localization of these sites, although some information has been accumulated over the last few years. The anticoagulant-effect site is associated with two pairs of lysine residues between positions 54 and 77 (the 'pancreatic' loop; Kini & Evans, 1989; Carredano *et al.*, 1998). In the structure of toxin RVV-VD from Russell's viper (Carredano *et al.*, 1998) four lysine residues were observed at positions 54, 56, 67 and 69 which might be associated with anticoagulant action. The myotoxic and Ca^{2+}-independent membrane-damaging activities have been associated with the C-terminal region of Lys49-PLA_2s (Ward *et al.*, 2002; Chioato *et al.*, 2002). Recently, site-directed mutagenesis experiments (Chioato *et al.*, 2002) showed these activities to be independent and determined by discrete yet partially overlapping motifs in the C-terminal loop, where residue Lys122 is essential for this function. Recent structural results also support this hypothesis (Magro *et al.*, 2003; Lee *et al.*, 2001). However, no structural information is known about the hypotensive effect and only a hypothesis has been developed for the inhibition of platelet aggregation (Wang *et al.*, 1996) in which it was suggested that the aromatic cluster formed by Phe20, Trp21 ('short' helix) and Phe113 and Trp119 (C-terminal) residues might be responsible for the platelet-aggregation inhibition effect. However, these aromatic residues are not totally conserved in some PLA_2s which also possess this activity.

BthA-I chemically modified with BPB shows an interesting characteristic after inhibitor binding: oligomeric change. While the native protein appears to be a monomer or a weakly formed dimer, the BPB-modified protein appears to be a more energetically and conformationally stable dimer structure. Furthermore, this 'new' oligomeric structure of BthA-I–BPB buries a large number of residues in the dimeric interface which includes key regions related to the pharmacological effects for PLA_2s: the C-terminal loop, the 'short' helix and Lys69 (which belongs to the 'pancreatic loop' in class I PLA_2s and is associated with anticoagulant activities in class II PLA_2s). It has been proposed (Carredano *et al.*, 1998) that this residue is essential for the anticoagulant effect. Lys69 from both BthA-I–BPB monomers makes hydrogen bonds with C-terminal residues (Fig. 2). Consequently, we suggest that BPB binding may indirectly inhibit the anticoagulant effect and possibly other pharmacological effects such as hypotensive and platelet-aggregation inhibition by oligomeric structural changes.

In conclusion, modification of BthA-I by BPB leads to both tertiary and quaternary structural changes. The novel oligomeric conformation is more stable when compared with the native structure and the inhibition of pharmacological effects by the ligand might arise from the oligomeric changes in the protein structure. Further structural studies, including site-directed mutagenesis, must be performed to understand the pharmacological activities of this and other PLA_2s in order to aid the design of specific and potent inhibitors which could lead to new drugs.

This work was supported by Fundação de Amparo à Pesquisa do Estado de São Paulo (FAPESP), Conselho Nacional de Desenvolvimento Científico e Tecnológico (CNPq), Fundação para o Desenvolvimento da UNESP (FUNDUNESP) and Laboratório Nacional de Luz Síncrontron (LNLS, Campinas-SP).

References

Andrião-Escarso, S. H., Soares, A. M., Fontes, M. R. M., Fuly, A. L., Corrêa, F. M. A., Rosa, J. C., Greene, L. J. & Giglio, J. R. (2002). *Biochem. Pharmacol.* **64**, 723–732.

Arni, R. K., Fontes, M. R. M., Barberato, C., Gutiérrez, J. M., Díaz-Oreiro, C. & Ward, R. J. (1999). *Arch. Biochem. Biophys.* **366**, 177–182.

Azevedo, W. F. de, Ward, R. J., Lombardi, F. R., Giglio, J. R., Soares, A. M., Fontes, M. R. M. & Arni, R. K. (1997). *Protein Pept. Lett.* **4**, 329–334.

Brünger, A. T., Adams, P. D., Clore, G. M., DeLano, W. L., Gros, P., Grosse-Kunstleve, R. W., Jiang, J.-S., Kuszewski, J., Nilges, M., Pannu, N. S., Read, R. J., Rice, L. M., Simonson, T. & Warren, G. L. (1998). *Acta Cryst.* D**54**, 905–921.

Carredano, E., Westerlund, B., Persson, B., Saarinen, M., Ramaswamy, S., Eaker, D. & Eklund, H. (1998). *Toxicon*, **36**, 75–92.

Carson, M. (1997). *Methods Enzymol.* **277**, 493–505.

Chandra, V., Kaur, P., Jasti, J., Betzel, C. & Singh, T. P. (2001). *Acta Cryst.* D**57**, 1793–1798.

Chioato, L., de Oliveira, A. H., Ruller, R., Sá, J. M. & Ward, R. J. (2002). *Biochem. J.* **366**, 971–976.
Daniele, J. J., Bianco, I. D. & Fidelio, G. D. (1995). *Arch. Biochem. Biophys.* **318**, 65–70.
Deenen, L. L. M. van & de Haas, G. H. (1963). *Biochem. Biophys. Acta*, **70**, 538–553.
DeLano, W. L. (2002). *The PyMOL Molecular Graphics System.* DeLano Scientific, San Carlos, USA.
Georgieva, D. N., Rypniewski, W., Gabdoulkhakov, A., Genov, N. & Betzel, C. (2004). *Biochem. Biophys. Res. Commun.* **319**, 1314–1321.
Gutiérrez, J. M. & Lomonte, B. (1997). *Venom Phospholipase A_2 Enzymes: Structure, Function and Mechanism*, edited by R. M. Kini, pp. 321–352. Chichester: Wiley & Sons.
Homsi-Brandeburgo, M. I., Queiroz, L. S., Santo-Neto, H., Rodrigues-Simioni, L. & Giglio, J. R. (1988). *Toxicon*, **26**, 615–627.
Jancarik, J. & Kim, S.-H. (1991). *J. Appl. Cryst.* **24**, 409–411.
Jones, T. A., Bergdoll, M. & Kjeldgaard, M. (1990). *Crystallographic and Modelling Methods in Molecular Design*, edited by C. E. Bugg & S. E. Ealick, pp. 189–195. New York: Springer-Verlag.
Kini, R. M. & Evans, H. J. (1989). *Toxicon*, **27**, 613–635.
Kleywegt, G. J. & Jones, T. A. (1997). *Methods Enzymol.* **277**, 208–230.
Laskowski, R. A., MacArthur, M. W., Moss, D. S. & Thornton, J. M. (1993). *J. Appl. Cryst.* **26**, 283–291.
Lee, W. H., da Silva-Giotto, M. T., Marangoni, S., Toyama, M. H., Polikarpov, I. & Garratt, R. C. (2001). *Biochemistry*, **40**, 28–36.
MacPherson, A. (1982). *Preparation and Analysis of Protein Crystals.* New York: Wiley.
Magro, A. J., Murakami, M. T., Marcussi, S., Soares, A. M., Arni, R. K. & Fontes, M. R. M. (2004). *Biochem. Biophys. Res. Commun.* **323**, 24–31.
Magro, A. J., Soares, A. M., Giglio, J. R. & Fontes, M. R. M. (2003). *Biochem. Biophys. Res. Commun.* **311**, 713–720.
Navaza, J. (1994). *Acta Cryst.* A**50**, 157–163.
Otwinowski, Z. & Minor, W. (1997). *Methods Enzymol.* **276**, 307–326.
Ownby, C. L. (1998). *J. Toxicol. Toxin Rev.* **17**, 1003–1009.
Pereira, M. F., Novello, J. C., Cintra, A. C. O., Giglio, J. R., Landucci, E. C. T., Oliveira, B. & Marangoni, S. (1998). *J. Protein Chem.* **17**, 381–386.
Renetseder, R., Dijkstra, B. W., Huizunga, K. H., Kalk, K. H. & Drenth, J. (1988). *J. Mol. Biol.* **200**, 181–188.
Rigden, D. J., Hwa, L. W., Marangoni, S., Toyama, M. H. & Polikarpov, I. (2003). *Acta Cryst.* D**59**, 255–262.
Roberto, P. G., Kashima, S., Marcussi, S., Pereira, J. O., Astolfi-Filho, S., Nomizo, A., Giglio, J. R., Fontes, M. R. M., Soares, A. M. & França, S. C. (2004). *Protein J.* **23**, 273–285.
Roberto, P. G., Kashima, S., Soares, A. M., Chioato, L., Faça, V. M., Fuly, A. L., Astolfi-Filho, S., Pereira, J. O. & França, S. C. (2004). *Protein Expr. Purif.* **37**, 102–108.
Rosenberg, P. (1990). *Handbook of Toxinology*, edited by W. Shier & D. Mebs, pp. 67–277. New York: Marcel Dekker.
Scott, D. L., White, S. P., Otwinowski, Z., Yuan, W., Gelb, M. H. & Sigler, P. B. (1990). *Science*, **250**, 1541–1546.
Serrano, S. M. T., Reichl, A. P., Mentele, R., Auerswald, E. A., Santoro, M. L., Sampaio, C. A. M., Camargo, A. C. M. & Assakura, M. T. (1999). *Arch. Biochem. Biophys.* **367**, 26–32.
Silva-Giotto, M. T. da, Garratt, R. C., Oliva, G., Mascarenhas, Y. P., Giglio, J. R., Cintra, A. C. O., de Azevedo, W. F. Jr, Arni, R. K. & Ward, R. J. (1998). *Proteins*, **30**, 442–454.
Six, D. A. & Dennis, E. A. (2000). *Biochim. Biophys. Acta*, **1488**, 1–19.
Soares, A. M., Fontes, M. R. M. & Giglio, J. R. (2004). *Curr. Org. Chem.* **8**, 1677–1690.
Soares, A. M. & Giglio, J. R. (2003). *Biochemie*, **42**, 855–868.
Takeda, A. A. S., dos Santos, J. I., Marcussi, S., Silveira, L. B., Soares, A. M. & Fontes, M. R. M. (2004). *Biochim. Biophys. Acta*, **1699**, 281–284.
Valentin, E. & Lambeau, G. (2000). *Biochimie*, **82**, 815–831.
Volwerk, J. J., Pieterson, W. A. & de Haas, G. H. (1974). *Biochemistry*, **13**, 1446–1454.
Wallace, A. C., Laskowski, R. A. & Thornton, J. M. (1995). *Protein Eng.* **8**, 127–134.
Wang, X., Yang, J., Gui, L., Lin, Z., Chen, Y. & Zhou, Y. (1996). *J. Mol. Biol.* **255**, 669–676.
Ward, R. J., Chioato, L., Oliveira, A. H. C., Ruller, R. & Sá, J. M. (2002). *Biochem. J.* **366**, 971–976.
Watanabe, L., Soares, A. M., Ward, R. J., Fontes, M. R. M. & Arni, R. K. (2005). *Biochimie*, **87**, 161–167.
Zhang, X., Zheng, L., Lin, N. Q., Ruan, K. C. & Zhou, Y. C. (1994). *Chin. Biochem. J.* **10**, 330–334.
Zhao, H., Liang, T., Xiaoqiang, W., Yuancong, Z. & Zhengjiong, L. (1998). *Toxicon*, **36**, 875–886.